

# Evaluating Nonlinearity on Granular Materials and Soils Through the Use of Deflection Techniques

Fabricio Leiva-Villacorta, Luis Loría-Salazar  
and Edgar Camacho-Garita

**Abstract** The nonlinear behavior of soils and granular materials is widely known. Its proper evaluation is essential for the accurate determination of the stiffness of pavement layers and their structural evaluation. If this phenomenon is not considered appropriately, it can lead to significant errors in estimating the pavement responses. As part of the investigation of accelerated tests on full-scale pavements by the National Laboratory of Materials and Structural Models of the University of Costa Rica, four instrumented pavement sections were built and evaluated using a Heavy Vehicle Simulator. The wheel load was used at an average speed of 10 km/h, with various loading levels, at an average temperature of 23 °C and with a lateral wandering of 10 cm. The deflection profile of each pavement was studied by means of Multi-Depth Deflectometer sensors (MDDs), the Road Surface Deflectometer (RSD), and; the Falling Weight Deflectometer (FWD). This paper summarizes a comparison among the differences in the deflection basin measurements, and the related estimated moduli. Additionally, the pavement response modeling was performed by means of Multi-layer Elastic (MLE), Finite Element (FE) and Linear Visco-Elastic (LVE) methods. The objective of this study was to compare the results of different deflection measuring methods and their correspondent backcalculated moduli. The analysis showed similar results in the deflection curves and hence, back-calculated moduli obtained by the MDDs and the RSD. Both devices captured, as expected, nonlinear behavior of the granular materials as well as the subgrade. The FWD was not able to report such behavior.

---

F. Leiva-Villacorta (✉) · L. Loría-Salazar · E. Camacho-Garita  
National Laboratory of Materials and Structural Models (LanammeUCR),  
University of Costa Rica, P.O. Box 11501-2060, San José, Costa Rica  
e-mail: fabricio.leiva@ucr.ac.cr

L. Loría-Salazar  
e-mail: luis.loriasalazar@ucr.ac.cr

E. Camacho-Garita  
e-mail: edgar.camachogarita@ucr.ac.cr

## 1 Introduction

It is generally known that unbound materials have a non-linear elastic stress-strain behavior. Because the unbound base courses have a substantial influence on the load carrying capacity of the pavements, proper characterization of the mechanical response of unbound aggregate materials is a crucial factor. In flexible pavements granular layers play an important role in the overall performance of the pavement. Consequently, to establish more rational pavement design and construction criteria, it is essential that the response of unbound layers under traffic loading be thoroughly understood.

Accurate stiffness (modulus) characterization of the unbound layers is critical for accurate pavement layer thickness design. For any mechanistically based pavement design, an accurate knowledge of the strains at critical locations in the pavement structure are necessary to give a quality prediction of the design life of that pavement.

Often, the stiffness of the unbound materials is quantified as the resilient modulus. Resilient modulus is the ratio of deviatoric stress (from a triaxial compression test) to recoverable strain. This term is utilized since unbound material behavior is not completely elastic; these materials usually experience some permanent deformation after each load application. Unbound material resilient moduli can be determined either in the laboratory using the triaxial testing apparatus or in the field using a variety of non-destructive testing methods. The laboratory resilient modulus test calculates resilient modulus by directly measuring the load and deformation of the test specimen under repeated loadings that simulate the quick loads imparted on the pavement structure by moving traffic. One of the most common field tests for resilient modulus is done with a falling weight deflectometer (or FWD).

The resilient moduli of unbound paving materials often exhibit non-linear stress dependent behavior with varying stress-states within the material (Irwin 2002). This behavior can either be stress-hardening (increasing stiffness with increasing stress) or stress-softening (decreasing stiffness with increasing stress) (Irwin 2002). Research into unbound material performance through laboratory and field testing has yielded several constitutive relationships relating resilient modulus to stress-state. These models contain a wide range of terms that quantify the stress-state of the unbound materials, such as: bulk stress ( $\theta$ ), deviatoric stress ( $\sigma_d$ ), and octahedral shear stress ( $\tau_{oct}$ ).

In order to effectively characterize the stiffness behavior of unbound materials, several factors must be considered. A better representation of material behavior can be given by either laboratory or field resilient modulus testing or both. The unbound material is stress-sensitive; therefore, a model that best quantifies the behavior of that material should be selected. Taking these factors into account could allow for the most accurate quantification of resilient modulus for pavement design and more accurate modeling of pavement design life. For many researchers and transportation agencies, these factors can be analyzed through full-scale accelerated pavement testing (APT).

One such facility is the Costa Rican APT program call PaveLab. A technical and economical study was performed and aided in determining that the Heavy Vehicle Simulator (HVS) was the best fit for the medium and long term pavement performance assessment. Specifically, the HVS met the following mobility, accelerated pavement evaluation, application of real loads and comparable results from similar equipments (Coetzee et al. 2008). Part of the testing program at the PaveLab involves characterization of the various paving layer materials in both the laboratory and the field, making this facility ideal for a study of this nature.

### 1.1 PaveLab Test Tracks

For the first stage of accelerated tests in Costa Rica the construction of 4 experimental sections was performed in May 2013 (Fig. 1). The objective of this phase was to perform a structural comparison in terms of thickness of the asphalt concrete layer and base material type (granular vs. cement treated) (Aguiar-Moya et al. 2012). Table 1 shows the characteristics of the 4 sections with their respective layer thicknesses obtained from Ground Penetrating Radar (GPR) measurements and backcalculated layer moduli based on Falling Weight Deflectometer results. The top layer consists of an asphalt concrete mixture with nominal maximum aggregate size of 19.0 mm with an optimum binder content of 4.9 % by total weight of mixture. The cement treated base (CTB) was designed to withstand 35 kg/cm<sup>2</sup> with an optimum cement content of 1.7 % by volume of aggregate and with a maximum density of 2013 kg/m<sup>3</sup>. The base material and granular sub-base were placed at a maximum density of 2217 kg/m<sup>3</sup> with an optimum moisture content of 8.6 %. The sub-base material had a CBR of 95 %. Finally, the subgrade material was constructed for a maximum density of 1056 kg/m<sup>3</sup> with an optimum moisture content of 52 % and CBR of 6.6 %.

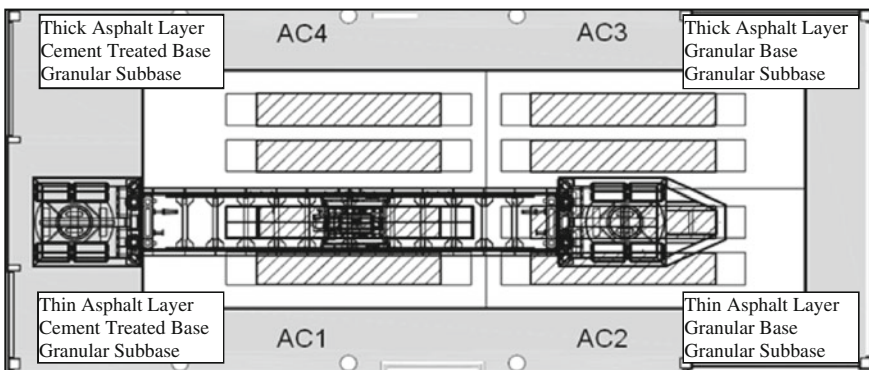


Fig. 1 Test track distribution

**Table 1** Test tracks in-place properties

Properties\section	AC1	AC2	AC3	AC4
Asphalt concrete thickness (H1) (cm)	5.1	6.3	13.2	13.2
Base thickness (H2) (cm)	21.9	21.2	31.0	24.9
Subbase thickness (H3) (cm)	30.1	30.1	30.1	30.1
HMA modulus (E1) @ 25 °C (MPa)	3800	3800	3800	3800
Base modulus (E2) (MPa)	1200	170	170	1200
Subbase modulus (E3) (MPa)	140	140	140	140
Subgrade modulus (E4) (MPa)	70	70	70	70

### 1.2 Instrumentation

The experiment included not only the instrumentation integrated with the HVS system but also embedded instrumentation in all four test sections. HVS onboard sensors can record the applied load, tire pressure and temperature, position of the load and the velocity of the load carriage. Embedded instrumentation include asphalt strain gauges (PAST model sensors), pressure cells (SOPT model sensors), multi depth deflectometers (MDD), moisture and temperature probes. These sensors were chosen based on previous HVS owners experience (Baker et al. 1994). Additionally, the HVS was equipped with a laser profiler that can be used to create a tridimensional profile of the section and a Road Surface Deflectometer is added to the testing equipment to obtain deflection basins at any location along the test section (Leiva-Villacorta et al. 2013, 2015).

Figure 2 shows the instrumentation array used for the first series of experimental sections. The PAST sensors were placed at the base/HMA layer interface and were placed in the longitudinal or traffic loading direction and in the transverse direction. MDD sensors were installed at 4 different depths to cover all 4 structural layers. As for the thermocouples, these were placed at 4 depths: surface, middle depth of the HMA layer, at the PAST sensors depth and 5 cm into the base layer. In the case of AC1 and AC3 sections the same gauge array was used while excluding PAST

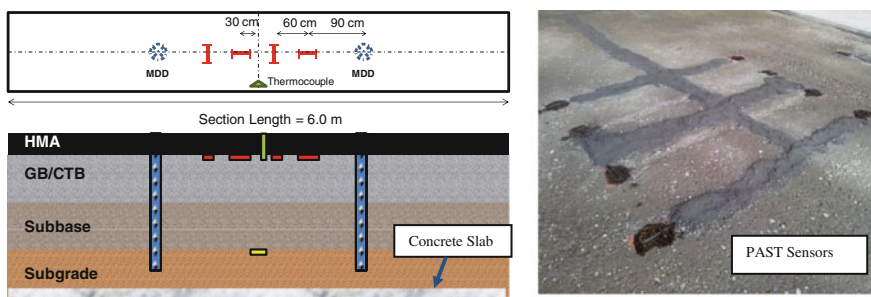


**Fig. 2** Sensor array

sensors. The Road Surface Deflectometer (RSD) was used to measure deflections at other locations along each section.

### 1.3 Surface Modulus as Indicator of Non-linear Behavior

The surface modulus is the ‘weighted mean modulus’ of the semi-infinite space calculated from the surface deflection using Boussinesq’s equations (Ullidtz 1987). The surface modulus at a distance ‘r’ roughly reflects the surface modulus at the same equivalent depth  $z = r$ . If the subgrade is a linear elastic semi-infinite space, the surface modulus should be the same at varying distances. If a stiff layer is present, the surface modulus at some distance should become very large. The surface modulus (SM) directly under the point of loading at maximum deflection  $D_0$  is calculated with Eq. 1, the general formula for surface modulus (SM) at any point away from the point of maximum deflection is calculated with Eq. 2.

$$SM = 2\sigma_0(1 - \mu^2) \left( \frac{a}{d_0} \right) \quad (r = 0) \quad (1)$$

$$SM = \sigma_0(1 - \mu^2) \left( \frac{a^2}{rd_r} \right) \quad (2)$$

where,

SM = Surface modulus at a distance r from centre of loading plate (MPa)

$\sigma$  = Contact stress

$\mu$  = Poisson’s ratio, usually chosen as 0.35

a = Radius of the loading plate

d(r) = Deflection at distance r

r = Radial distance from the centre of loading where  $r > 0$ .

Ullidtz (1987, 2005) determined that the gradient of the surface modulus (SM) plot over more or less the radial distance away of the deflection bowl can be used to identify whether the subgrade has stress softening, stress hardening behavior or whether it is exhibiting linear elastic behavior. Figure 3 shows what it can be defined as linear elastic behavior (on the left) and non-linear elastic behavior/rigid layer effect. The “kick” in the surface modulus plot (Fig. 3—right) could be caused by a shallow rigid layer (bedrock) or nonlinear (stress softening) materials such as clay will cause a similar effect in the deflection basins.

Leiva-Villacorta et al. (2015) performed an analysis of deflection basins using surface modulus theory. Their results indicated that before APT test loads were applied to one test track, FWD deflection basins most likely reflected an elastic linear behavior of the lower layers while RSD and MDD reflected a moderately non-linear elastic behavior. Furthermore, a similar surface modulus analysis performed at the end of APT testing, indicated that FWD results consistently reflect an elastic linear behavior of the lower layers, while RSD and MDD reflect a more

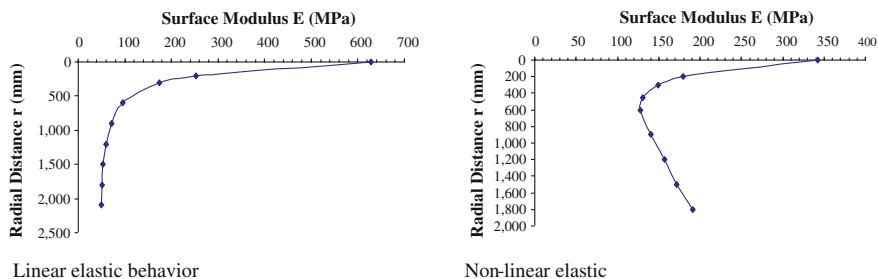


**Fig. 3** Typical surface moduli plots for pavement structures

intensified non-linear behavior of the lower layers and could also exhibit the presence of the test pit concrete support layer (shallow rigid layer). Therefore, a more in depth study was recommended in order to explain the differences in the observed behavior based on the different deflection measurement devices.

#### 1.4 Objective

The objective of this study was to analyze and compare measured and modeled surface deflection basins to try explain the linear and non-linear behavior of the unbound layers captured by different devices.

In order to achieve the objective of this study, Multi-layer Elastic (MLE), Finite Element (FE) and Linear Visco-Elastic (LVE) modeling was used to compute surface deflections based on linear elastic properties of the four pavement structures and non-linear elastic properties of the unbound layers. On the other hand, FWD deflection basins at different load levels that were performed on the four test tracks located at Lanamme's APT facility were evaluated. Deflections obtained from surface MDD sensors and the RSD testing at different load levels and locations were analyzed as well. Finally, computed and measured results were compared and the linear elastic/non-linear behavior was defined based on surface modulus plots and benchmark parameters.

## 2 Pavement Modeling

The pavement response modeling was performed by means of Multi-layer Elastic (MLE), Finite Element (FE) and Linear Visco-Elastic (LVE) methods. The pavement structure was firstly simulated considering the subgrade as semi-infinite layer and secondly considering the actual 40 cm concrete slab located at a depth of 2.8 m. The simulated elastic modulus of concrete slab was 8 000 MPa and it was expected to behave as a shallow bed rock. A single circular load with uniform

pressure distribution was used to compute surface deflections at the same locations of the FWD sensors and the FWD load configuration (plate diameter = 300 mm). Two loads were simulated 40 and 60 kN for all four sections.

The surface modulus differential (SMD) defined as the difference between the surface modulus at 600 mm and that at 1200 mm was used to discriminate between linear and non-linear behavior. This concept was introduced by Horak (2008). Horak (2008) defined ranges of the SMD as benchmark of the unbound layers response as either stress softening behavior ( $SMD < -20$ ), stress stiffening behavior ( $SMD > 20$ ) or linear elastic behavior ( $-20$  to  $20$ ). In addition, the concept of “kick” value was introduced in this study to perform further analyses. This value was defined as the difference between the surface modulus at 600 mm and that at 1800 mm. In theory, if the “kick” value was similar to the SMD the linear elastic behavior in the surface modulus plot can be confirmed, if the “kick” value was significantly different from the SMD a non-linear behavior would be plausible.

### 2.1 Multi-layer Elastic Modeling

Layer moduli were simulated using the backcalculated results exhibit in Table 1 for all four sections. The Multi-layer Elastic software PitraPave developed by LanammeUCR was used to estimate surface deflections. Figure 4 exhibits the computed deflections for each section and the associated surface modulus.

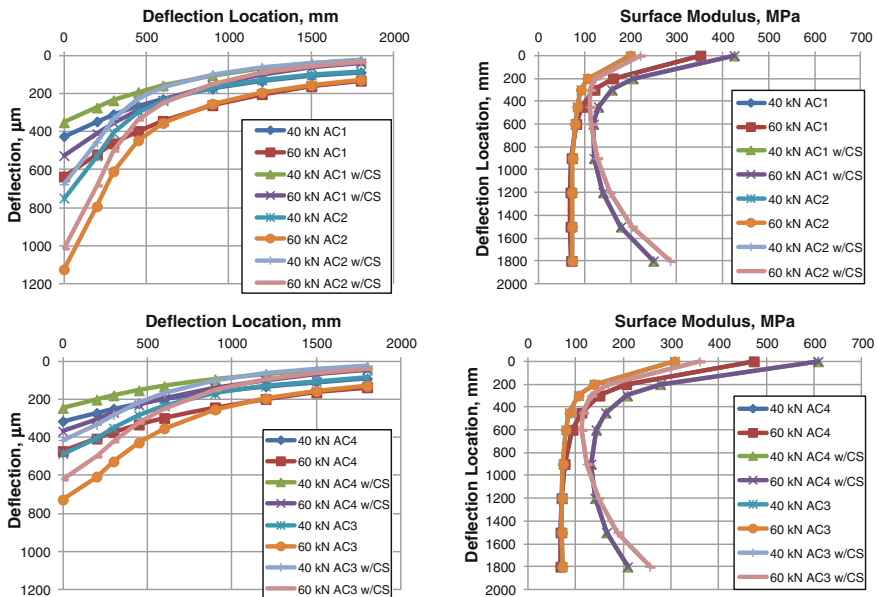


Fig. 4 Computed deflection basins and surface moduli

As expected, the section with the lowest structural capacity (AC2) presented the highest overall deflection and the section with the highest structural capacity (AC4) presented the lowest overall deflection. It was also expected to obtain the same surface modulus at any load level and to reflected an elastic linear behavior of the lower layers. However, the inclusion of the 40 cm concrete slab not only produced lower deflections but also produced a “kick” in the surface modulus plot which tended to be inversely proportional to the structural capacity of the pavement section. As expected, lower surface moduli near the center of the applied load indicated a lower supporting capacity of the upper layers.

The surface modulus differential (SMD) and the “kick” parameter were calculated for each section under the semi-infinite subgrade structure and the inclusion of the concrete slab. These results along with the maximum deflection (D0) and surface modulus at two different locations are shown in Table 2. The surface modulus at D0 represents the structural capacity of the upper layers while the SM at D1800, if a linear elastic behavior is observed, represents the modulus of the subgrade. This was the case for the semi-infinite subgrade simulated structure which yielded surface moduli around the assumed modulus of the subgrade (70 MPa). Moreover, when following the SMD criteria it was observed that all the sections but AC4 reflected a linear elastic behavior. In this case, section AC4 presented a stress stiffening behavior. The SMD and “kick” values were identical and both followed the same trend for the semi-infinite subgrade structure while a significant difference between these parameters was observed for the structure with the concrete slab. Based on the SMD criteria all sections but AC4 followed a non-linear behavior (stress softening). In this case, AC4 presented a linear elastic behavior based on the SMD concept. However, the “kick” value indicates that all sections presented a non-linear behavior (stress softening) as observed in Fig. 4.

## 2.2 *Finite Element Modeling*

Mechanistic analysis was performed using a non-linear finite element program called MichPave (Harichandran et al. 1990). The mechanistic analyses performed by MichPave includes the effect of gravity and lateral stresses arising from the weight of the materials. Displacements, stresses and strains due to a single circular wheel load are computed. Due to the assumptions used, the problem is reduced to an axisymmetric one. Layer elastic moduli were simulated using the backcalculated results exhibit in Table 1 for all four sections for the bounded layers. The resilient modulus for the granular base was specified in terms of the bulk stress through the  $k-\theta$  model (Eq. 3) and the resilient modulus for the cohesive soil was specified in terms of the deviatoric stress through the bilinear model (Eq. 4).



**Table 2** Surface modulus analysis under MLE modeling

Section	Semi-infinite subgrade					With concrete slab				
	D0 (mm)	SM@D0 (MPa)	SM@D1800 (MPa)	SMD (MPa)	Kick (MPa)	D0 (mm)	SM@D0 (MPa)	SM@D1800 (MPa)	SMD (MPa)	Kick (MPa)
AC1	424.0	351.3	70.4	12.5	11.0	350.8	424.7	248.9	-20.7	-130.2
AC2	749.5	198.8	73.2	6.4	5.5	676.2	220.3	285.5	-41.2	-172.4
AC3	484.7	307.4	72.2	7.5	7.1	413.9	359.9	255.0	-34.5	-142.3
AC4	314.6	473.6	68.3	23.0	25.4	245.0	608.1	208.8	2.3	-65.8

$$MR = 11.795 * (\theta)^{0.342} \tag{3}$$

where,

MR = Resilient Modulus (MPa)

$\theta$  = Bulk Stress (kPa)

$$MR = 82.5 + 0.310[48 - \sigma_d] \quad \text{when } (\sigma_d \leq 48)$$

$$MR = 82.5 - 0.192[\sigma_d - 48] \quad \text{when } (\sigma_d > 48) \tag{4}$$

where,

MR = Resilient Modulus (MPa)

$\sigma_d$  = Deviatoric Stress (kPa).

Figure 5 exhibits the computed deflections at a 40 kN load for each section and the associated surface modulus. The level of deflections and form of the surface modulus plots were consistent with the previous analyses. It was also expected to observe a non-linear trend of the simulated pavement structures with the semi-infinite subgrade layer. However, the plots seemed to reflect a linear elastic behavior despite the use of unbound material properties in the model. The inclusion of the 40 cm concrete slab not only produced lower deflections but also produced the “kick” in the surface modulus plot which tended to be inversely proportional to the structural capacity of the pavement section as well.

The results of the deflection and surface modulus analysis are shown in Table 3. In the case of the semi-infinite subgrade simulated structure, the simulation yielded surface moduli around the assumed modulus of the subgrade (70 MPa) for sections AC1 and AC4 and slightly higher values for sections AC2 and AC3. When following the SMD criteria it was observed that all the sections reflected a linear elastic behavior. The SMD and “kick” values were slightly different for sections AC2 and AC3 suggesting a low effect of the non-linear behavior of the unbound layers. Once again, a significant difference between these parameters was observed for the structure with the concrete slab. Based on the SMD criteria all sections but AC4 followed a non-linear behavior (stress softening). In this case, AC4 presented

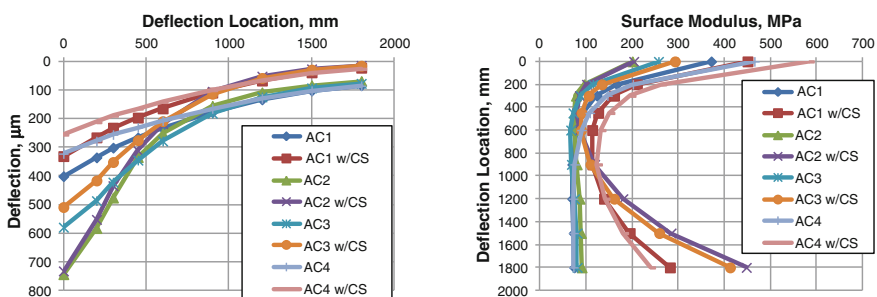


Fig. 5 Computed deflection basins and surface moduli @ 40 kN load

**Table 3** Surface modulus analysis under FEA modeling

Section	Semi-infinite subgrade					With concrete slab				
	D0 (mm)	SM@D0 (MPa)	SM@D1800 (MPa)	SMD (MPa)	Kick (MPa)	D0 (mm)	SM@D0 (MPa)	SM@D1800 (MPa)	SMD (MPa)	Kick (MPa)
40 kN AC1	401.3	371.3	74.4	9.7	5.4	331.0	450.1	281.9	-25.7	-168.5
60 kN AC1	595.5	375.2	74.3	10.2	6.2	490.5	455.6	280.0	-24.9	-165.3
40 kN AC2	743.8	200.3	90.6	-12.0	-16.5	732.3	203.4	447.4	-94.2	-361.8
60 kN AC2	1112.0	200.9	80.2	-11.8	-14.9	1002.5	222.9	437.7	-89.4	-350.4
40 kN AC3	579.5	257.1	80.8	-8.1	-13.9	509.0	292.7	412.0	-71.6	-322.8
60 kN AC3	844.3	264.7	80.5	-7.3	-12.9	738.3	302.7	402.9	-69.5	-312.4
40 kN AC4	322.3	462.3	72.9	17.8	17.0	255.5	583.0	239.0	-8.8	-107.4
60 kN AC4	480.5	465.0	72.8	18.2	17.6	380.8	586.9	238.0	-8.2	-105.5

a linear elastic behavior based on the SMD concept. However, the “kick” value indicated that all sections presented a non-linear behavior (stress softening). In the case of MLE modeling, the estimated surface moduli were the same for the two load levels. However, in this case a small change in the estimated values were obtained due to the non-linear response of the unbound layers to different stress states.

### 2.3 Linear Visco-Elastic Modeling

A single circular load with uniform pressure distribution was modeled using *3D-Move Analysis\_V2* (Asphalt Research Consortium 2014). The tool accounts for moving traffic loads with complex contact stress distributions of any shape, vehicle speed, and viscoelastic properties of asphalt concrete layers to calculate pavement responses using a continuum-based finite-layer approach. A dynamic analysis (10 kph) was performed using viscoelastic properties for the asphalt concrete layer obtained from dynamic modulus test results. For the remaining materials, only a linear elastic behavior can be modeled and the respective layer moduli are shown on Table 1. The dynamic modulus master curve is shown in Eq. 5. The laboratory results were obtained following AASHTO TP 79-11.

$$\log|E^*| = 0.1787 + \frac{3.526}{1 + e^{-1.444 + -0.5139\{\log \omega + \frac{197674}{19.14714}[(\frac{1}{T}) - (\frac{1}{T_r})]\}}}$$
(5)

where,

E\* = Dynamic modulus (ksi)

ω = Frequency (Hz)

T = Analysis temperature (296.15 K)

Tr = Reference temperature (294.15 K).

Figure 6 exhibits the computed deflections at a 40 kN load for each section and the associated surface modulus. It was expected to observe a linear elastic trend of

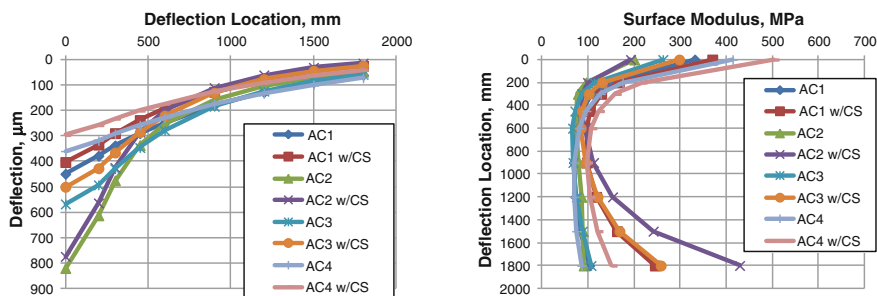


Fig. 6 Computed deflection basins and surface moduli @ 40 kN load

**Table 4** Surface modulus analysis under VEA modeling

Section	Semi-infinite subgrade					With concrete slab				
	D0 (mm)	SM@D0 (MPa)	SM@D1800 (MPa)	SMD (MPa)	Kick (MPa)	D0 (mm)	SM@D0 (MPa)	SM@D1800 (MPa)	SMD (MPa)	Kick (MPa)
40 kN AC1	449.4	331.5	102.9	0.6	-27.8	403.1	369.6	245.2	-21.3	-148.5
60 kN AC1	671.8	332.6	108.8	0.6	-31.1	604.6	369.6	249.7	-22.9	-153.0
40 kN AC2	820.0	181.7	130.7	-15.1	-57.3	774.0	192.5	428.8	-59.7	-335.1
60 kN AC2	1270.4	175.9	121.4	-13.2	-51.0	1161.2	192.4	428.8	-61.4	-336.8
40 kN AC3	567.7	262.4	106.6	-8.3	-39.8	500.3	297.7	257.8	-36.3	-173.3
60 kN AC3	811.8	275.3	114.9	-9.5	-44.5	750.5	297.7	257.8	-36.3	-173.3
40 kN AC4	360.0	413.8	85.9	11.9	-4.3	296.2	502.9	151.5	3.8	-43.8
60 kN AC4	540.0	413.8	85.9	11.9	-4.3	444.3	502.9	151.5	3.8	-43.8

the simulated pavement structures with the semi-infinite subgrade layer. However, the plots seemed to reflect a low intensity non-linear behavior despite the use of linear elastic modulus for the unbound layers. The inclusion of the 40 cm concrete slab not only produced lower deflections but also produced the “kick” in the surface modulus plot which tended to be inversely proportional to the structural capacity of the pavement section as well.

The results of the deflection and surface modulus analysis are shown in Table 4. In the case of the semi-infinite subgrade simulated structure, the simulation yielded surface moduli higher than the assumed modulus of the subgrade (70 MPa) for all sections. When following the SMD criteria it was observed that all the sections reflected a linear elastic behavior. The SMD and “kick” values were significantly different for all sections but AC4. These results suggested a non-linear behavior of the unbound layers. Once again, a significant difference between these parameters was observed for the structure with the concrete slab. Based on the SMD criteria all sections but AC4 followed a non-linear behavior (stress softening). AC4 presented a linear elastic behavior based on the SMD concept. However, the “kick” value indicated that all sections presented a non-linear behavior (stress softening). In this case, small changes in the estimated values were obtained between load levels due to the viscoelastic response of the asphalt concrete layer to different stress/strain states for all sections excluding AC4.

### 3 FWD Test Results

FWD testing was performed on each section, at three different locations, prior to the application of the accelerated loading. Deflection basins were obtained at three different load levels, approximately 40, 53 and 70 kN. Figure 7 exhibits the average of the three measured deflection basins for each section and the associated surface modulus. The surface modulus plots seemed to reflect a linear elastic behavior despite the use of unbound material with non-linear properties, despite the existence of the concrete slab and the apparent non-linear behavior induced by viscoelastic properties of the asphalt concrete.

The results of the deflection and surface modulus analysis are shown in Table 5. When following the SMD criteria it was observed that all the sections reflected a linear elastic behavior; however, section AC4 followed a non-linear behavior (stress stiffening). The SMD and “kick” values were very similar in all cases and both followed the same trend thus confirming that the FWD was not able to report the expected non-linear behavior.

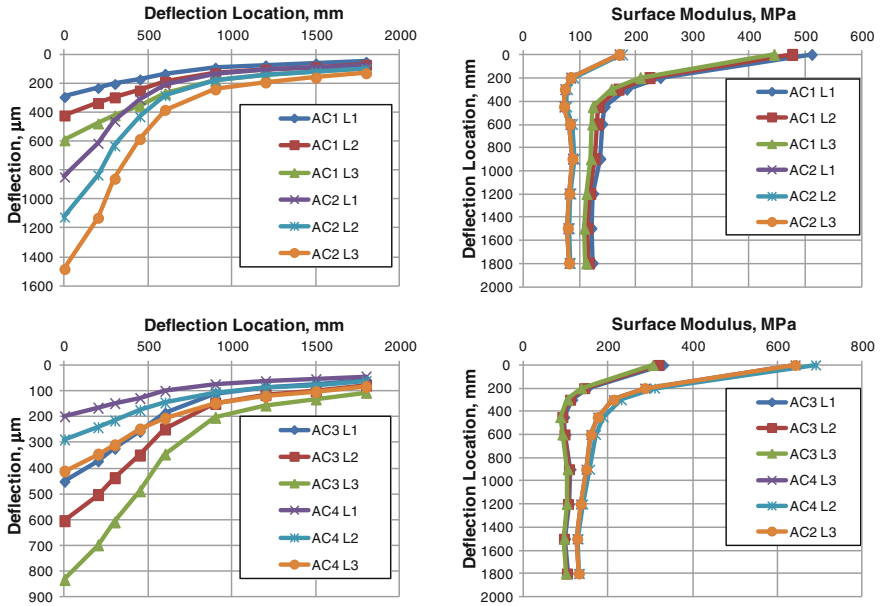


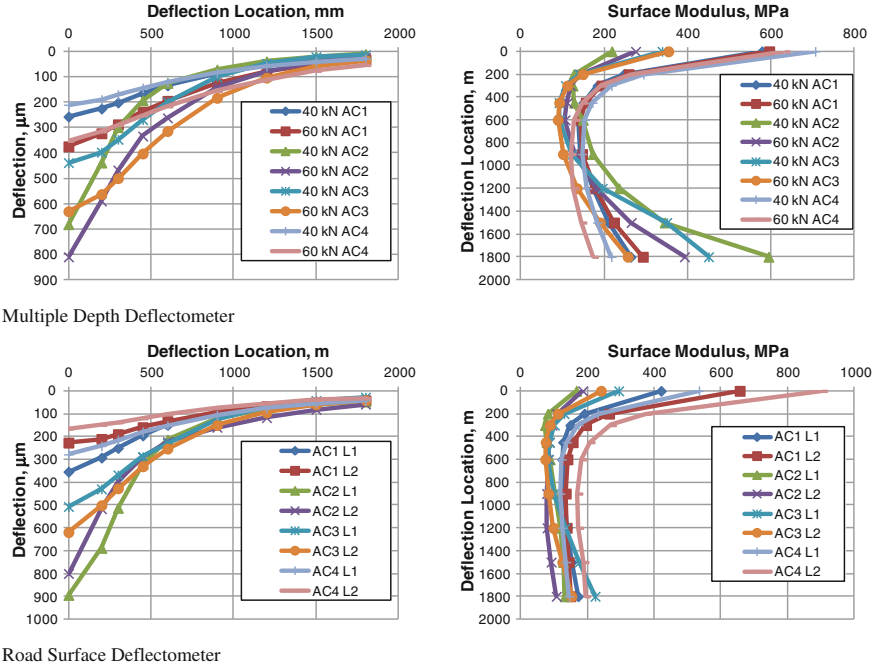
Fig. 7 Measured deflection basins and surface moduli from FWD results

Table 5 Surface modulus analysis for FWD results

Section	Load (kN)	D0 (mm)	SM@D0 (MPa)	SM@D1800 (MPa)	SMD (MPa)	Kick (MPa)
AC1	40.0	294.3	511.2	122.7	16.0	16.9
AC1	53.5	421.6	476.4	116.0	13.4	15.7
AC1	70.1	593.0	444.2	111.0	9.9	10.6
AC2	40.1	846.4	176.7	83.9	3.5	5.8
AC2	52.8	1123.0	175.3	82.6	2.8	4.0
AC2	67.5	1481.7	169.7	80.7	1.2	1.5
AC3	39.9	451.9	330.4	104.6	-8.5	-5.4
AC3	51.6	604.8	318.6	102.6	-8.2	-5.9
AC3	68.1	833.2	305.2	100.0	-10.2	-8.3
AC4	40.2	199.4	755.9	139.2	37.9	47.2
AC4	53.1	289.2	690.6	131.6	30.5	38.6
AC4	70.4	412.3	642.1	130.6	24.1	28.5

## 4 Multiple Depth Deflectometer and Road Surface Deflectometer Results

MDD sensors located at the surface of the pavement were used to measure deflection basins at two load levels (40 and 60 kN) prior to the actual load testing. RSD testing was performed on each section, at two different locations and at 40 kN,



**Fig. 8** Measured deflection basins and surface moduli from MDD and RSD

also prior to the application of the accelerated loading. Figure 8 exhibits the average measured deflection basins from three replicates for each section and the associated surface modulus. Both devices captured, as expected, nonlinear behavior of the granular materials as well as the subgrade. However, the RSD was able to report the expected non-linear behavior in a lower intensity compared to the MDDs.

The results of the deflection and surface modulus analysis are shown in Table 6. In the case of the MDD results, a small change in the surface moduli between load levels were obtained. This can be explained by the non-linear response of the unbound layers to different stress states and testing variability. Based on the SMD criteria, it was observed that all the sections reflected a linear elastic behavior. The SMD and “kick” values suggested a strong non-linear behavior of the unbound layers for sections AC1, AC2 and AC3. In the case of section AC4 the SMD criteria indicated a linear elastic response but the “kick” value and the surface modulus plot indicated a non-linear response.

A significant difference in the measured deflections were obtained for the RSD on sections AC1 and AC4 due to construction variability. Overall, the SMD and “kick” values suggested a mild non-linear behavior of the unbound layers for sections AC2 and AC3 and a mixed linear-elastic/non-linear behavior for section AC1.



**Table 6** Surface modulus analysis for MDD and RSD results

Section	D0 (mm)	SM@D0 (MPa)	SM@D1800 (MPa)	SMD (MPa)	Kick (MPa)
<i>MDD</i>					
40 kN AC1	257.3	579.1	263.8	-35.4	-125.3
60 kN AC1	374.6	596.5	293.2	-35.6	-150.1
40 kN AC2	681.6	218.5	594.8	-86.4	-445.5
60 kN AC2	810.3	275.8	393.1	-74.2	-286.7
40 kN AC3	438.8	339.5	450.9	-102.1	-357.4
60 kN AC3	630.6	354.4	256.9	-45.7	-168.0
40 kN AC4	210.7	707.0	217.6	-5.3	-64.0
60 kN AC4	352.5	634.0	173.8	2.8	-44.9
<i>RSD</i>					
AC1 L1	354.0	420.8	172.1	-14.8	-47.9
AC1 L2	226.7	657.1	149.1	2.2	-8.9
AC2 L1	894.0	166.6	132.0	-32.4	-44.7
AC2 L2	800.1	186.2	106.7	4.1	-23.2
AC3 L1	506.6	294.0	223.1	-52.0	-141.6
AC3 L2	619.0	240.7	152.1	-24.6	-78.6
AC4 L1	278.4	535.0	145.2	-1.7	-22.7
AC4 L2	164.6	904.9	193.4	10.7	-10.2

### 5 Summary and Comparison of Results

A summary of the SMD values obtained from measurements and mechanistic analysis and the tendency with respect to the linear or non-linear behavior can be observed in Fig. 9. The linear elastic behavior was set between -20 and 20 based on the SMD criteria, below -20 and above 20 was defined the non-linear behavior

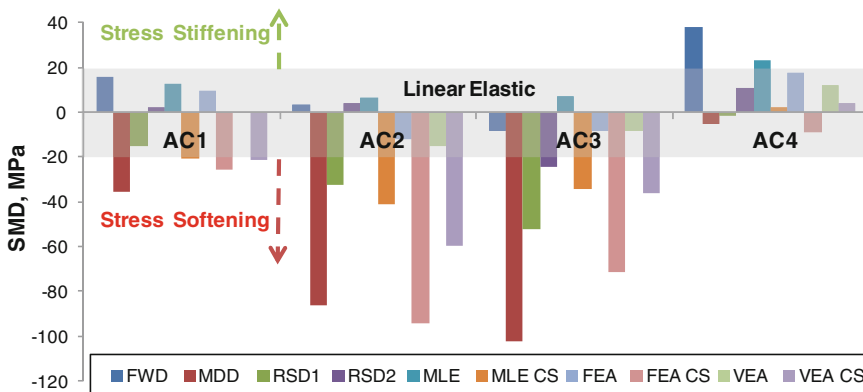


**Fig. 9** Summary of SMD results

region. In general, FWD results reflect an elastic linear behavior for sections AC1, AC2 and AC3 and reflect a stress stiffening behavior for section AC4. In agreement with this are the results from MLE considering a semi-infinite subgrade layer. MDD results reflect strong non-linear behavior for sections AC1, AC2 and AC3 and in agreement with this are the results from FEA when considering the concrete slab located at 2.8 m deep. RSD results reflect a mild non-linear behavior for sections AC2 and AC3 and in agreement with this are the results from MLE and VEA when considering the concrete slab located at 2.8 m deep. Finally, based on both, measured and predicted responses, it was determined that sections AC1 and AC4 presented mostly a linear elastic behavior and sections AC2 and AC3 followed, mostly a non-linear elastic behavior (stress softening) which was augmented by the presence of the concrete slab.

## 6 Conclusions

- The results observed with the MLE modeling suggested that the “kick” in a surface modulus plot could be caused by the shallow rigid layer (40 cm concrete slab) providing an apparent non-linear behavior.
- The results observed with the FEA modeling suggested that the “kick” in a surface modulus plot could be caused by the non-linear (stress softening/stiffening) behavior of the unbound materials. This non-linear behavior was intensified by the inclusion of the concrete slab.
- The results observed with the VEA modeling suggested that the “kick” in a surface modulus plot could be caused not only by a shallow rigid layer (bed-rock) or nonlinear (stress softening/stiffening) materials but also by the viscoelastic behavior of the asphalt concrete layer. This non-linear behavior was also intensified by the inclusion of the concrete slab.
- The results observed with the modeling of the 40 cm concrete slab located at a depth of 2.8 m indicated a significant change in the deflection basins and the surface modulus plots for all sections. This results suggest that a non-linear behavior should be observed when performing non-destructive testing on the evaluated pavement sections.
- FWD results consistently reflect an elastic linear behavior of the lower layers, while RSD and MDD reflect a more intensified non-linear behavior of the lower layers and could also exhibit the presence of the test pit concrete slab (shallow rigid layer).
- Finally, the new concept “kick” value defined as the difference between the surface modulus at 600 mm and that at 1,800 mm can be used as complement of the SMD value in order to discriminate between linear and non-linear behavior.

## References

- Aguiar-Moya, J. P., Corrales, J. P., Elizondo, F., & Loría-Salazar, L. (2012). PaveLab and heavy vehicle simulator implementation at the National Laboratory of Materials and Testing Models of the University of Costa Rica. In *Advances in pavement design through full-scale accelerated pavement testing*, APT 2012.
- Asphalt Research Consortium webpage. <http://www.arc.unr.edu/Software.html>. Date Accessed 03-20-2014.
- Baker Harris, B., Buth Michael, R., & Van Deusen David, A. (1994). *Minnesota road research project: Load response instrumentation installation and testing procedures*. Minnesota Department of Transportation.
- Coetzee, N., et al. (2008). The heavy vehicle simulator in accelerated pavement testing: Historical overview and new developments. In *3rd International Conference APT*.
- Harichandran, R. S., Yeh, M.-S., & Baladi, G. Y. (1990). MICH-PAVE: A nonlinear finite element program for the analysis of flexible pavements. *Transportation Research Record*, 1286, 123–131.
- Horak, E. (2008). Benchmarking the structural condition of flexible pavements with deflection bowl parameters. *Journal of the South African Institution of Civil Engineering*, 520(2), 2–9.
- Irwin, L. H. (2002). Backcalculation: An overview and perspective. In *Proceedings of the Pavement Evaluation Conference*. Roanoke, VA.
- Leiva-Villacorta, F., Aguiar-Moya, J. P., & Loria-Salazar, L. G. (2013). Ensayos acelerados de pavimento en Costa Rica. *Infraestructura Vial*, 15(26), 32–41.
- Leiva-Villacorta, F., Aguiar-Moya, J. P., & Loría-Salazar, L. G. (2015). Accelerated pavement testing first results at the Lanammeucr APT facility. In *Transportation Research Board 94th Annual Meeting*, Washington DC.
- Ullidtz, P. (1987). *Pavement analysis, development in civil engineering* (Vol. 19). Amsterdam: Elsevier.
- Ullidtz, P. (2005). *Modelling flexible pavement response and performance*. New York: Elsevier. ISBN 8750208055.